New Folder Name Mirror Orientation

LIGO PROJECT

CALIFORNIA INSTITUTE OF TECHNOLOGY

TO Distribution

DATE April 24, 1991

FROM Seiji Kawamura

EXT MAIL EMAIL

SUBJECT Mirror Orientation Noise in Interferometers

How the angle jitter of the cavity mirrors can be converted into interferometer displacement noise in the 40m prototype is analyzed. The experiment results confirming the model are shown. The predicted orientation noise is also shown.

Distribution:

A. Abramovici
M. Burka
R. Drever
A. Gillespie
Y. Gürsel
T. Lyons
F. Raab
M. Regehr
D. Shoemaker
L. Sievers
R. Spero
R. Vogt
R. Weiss
S. Whitcomb
M. Zucker

1. MIRROR ANGLE DEPENDENCE OF CAVITY LENGTH

In the cavity which consists of flat (M_1) and concave (M_2) mirrors like the 40m prototype (Fig.1), the cavity length along the beam axis (l) depends on each mirror angle (θ_1 for M_1 and θ_2 for M_2) as follows:

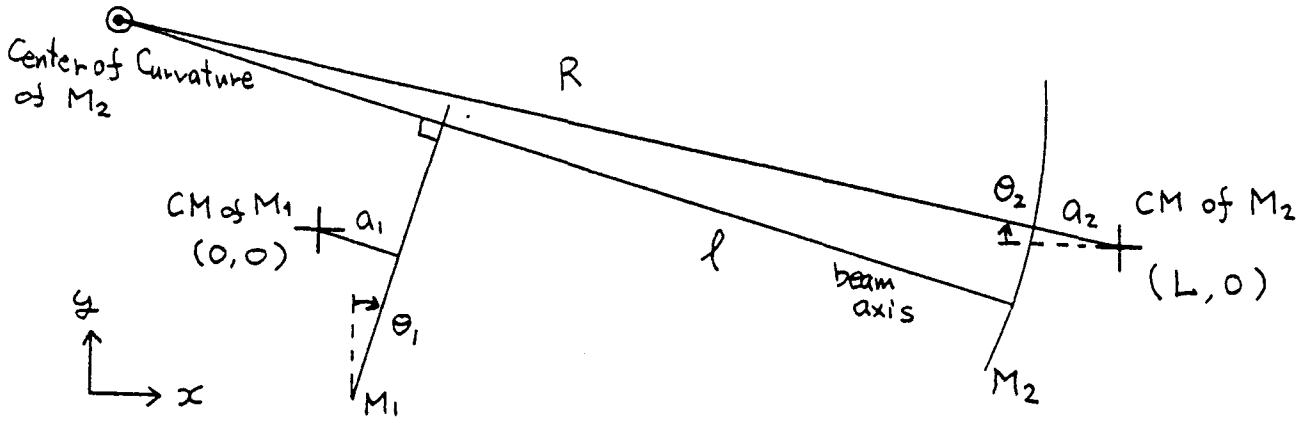

Fig. 1 Arm cavity of the 40m prototype

$$l = R - \sqrt{(x_1 - x_R)^2 + (y_1 - y_R)^2} \quad \cdots (1)$$

where (x_R, y_R) is the position of the curvature center of M_2, and (x_1, y_1) is that of the beam spot on M_1 in the coordinates of Fig.1;

$$x_R = L - (R + a_2)\cos\theta_2$$

$$y_R = (R + a_2)\sin\theta_2$$

$$x_1 = \frac{a_1 + L\tan^2\theta_1\cos\theta_1 + (R + a_2)\cos\theta_1\tan\theta_1(\sin\theta_2 - \tan\theta_1\cos\theta_2)}{\cos\theta_1(1 + \tan^2\theta_1)}$$

$$y_1 = \frac{(L\cos\theta_1 - a_1)\tan\theta_1 + (R + a_2)\cos\theta_1(\sin\theta_2 - \tan\theta_1\cos\theta_2)}{\cos\theta_1(1 + \tan^2\theta_1)}. \quad \cdots (2)$$

Here R is the radius of curvature of M_2, d_1 and d_2 are distances between the center mass and the mirror surface of M_1 and M_2, respectively, and L is the distance between two center masses.

To the second order of θ_1, θ_2,

$$l = (L - a_1 - a_2) + \frac{1}{2}(R + a_2 - L)\theta_1^2 + \frac{1}{2}(R + a_2)\theta_2^2 - (R + a_2)\theta_1\theta_2. \quad \cdots (3)$$

2. LINEAR EFFECT

(1) Theory

When each mirror has static offset angles (θ_{1st}, θ_{2st}) and small angle jitter ($\delta\theta_1$, $\delta\theta_2$);

$$\theta_1 = \theta_{1st} + \delta\theta_1$$
$$\theta_2 = \theta_{2st} + \delta\theta_2 \quad \cdots (4)$$

the corresponding cavity length variations (δl) are, from Eq.3, to the first order of $\delta\theta_1$, $\delta\theta_2$,

$$\delta l = d_{1st}\delta\theta_1 + d_{2st}\delta\theta_2 \quad \cdots (5)$$

where d_{1st} and d_{2st} are static distances between the beam axis and the center mass of M_1 and M_2, respectively;

$$d_{1st} = (R + a_2 - L)\theta_{1st} - (R + a_2)\theta_{2st}$$
$$d_{2st} = (R + a_2)\theta_{2st} - (R + a_2)\theta_{1st}. \quad \cdots (6)$$

(2) Experiment

The end mirror in the primary cavity of the 40m prototype (Huey) was used in tilt to investigate the problem.

Small angle jitter of the mirror ($\delta\theta$) were caused by applying a sinusoidal signal to the orientation coil at 250Hz, and the corresponding mirror displacement signals in the interferometer (δl) were measured as a function of static beam spot position on the mirror (d_{st}). The result is shown in Fig.2 with the theoretically predicted curve. They agree very well.

The linear effect was measured at several frequencies with the same d_{st}. The result shown in Table 1 indicates that there is no frequency dependence around the cavity pole frequency.

Table 1 Frequency dependence of the linear effect

Frequency [Hz]	20	50	100	250	500
$\delta l/\delta\theta$ [mm]	2.1	1.8	1.7	1.9	1.9

3. SIDEBAND EFFECT I

(1) Theory

When M_1 and M_2 angle fluctuates by $\Delta\theta_1$ and $\Delta\theta_2$ ($\sim \theta_{1,2st}$), respectively at a low frequency ω_A and in addition, M_2 angle jitters by $\delta\theta_2$ ($<< \theta_{1,2st}$) at ω_B ($>> \omega_A$);

$$\theta_1 = \theta_{1st} + \Delta\theta_1 \sin\omega_A t$$
$$\theta_2 = \theta_{2st} + \Delta\theta_2 \sin\omega_A t + \delta\theta_2 \sin\omega_B t \quad \cdots (7)$$

to the first order of $\delta\theta_2$, from Eq.3,

$$\delta l = d_{2st}\delta\theta_2 \sin\omega_B t + \frac{1}{2}\Delta d_2 \delta\theta_2 \{\cos(\omega_B - \omega_A) - \cos(\omega_B + \omega_A)\} \quad \cdots (8)$$

where Δd_2 is the $\Delta\theta_1$, $\Delta\theta_2$—caused fluctuation of the distance between the beam axis and the M_2 center mass ($\approx$ the beam spot fluctuation on M_2);

$$\Delta d_2 = (R + a_2)\Delta\theta_2 - (R + a_2)\Delta\theta_1. \quad \cdots (9)$$

The side band coupling with the beam spot fluctuation on M_2 appears at $\omega_B \pm \omega_A$ aside from the linear effect.

(2) Experiment

Large angle variations (1.6×10^{-6} rad_{rms}) at 10Hz and small angle variations (5.0×10^{-9} rad_{rms}) at 250Hz were artificially caused simultaneously, and the corresponding sideband displacement signal at 260Hz was measured to be 3.9×10^{-13} m_{rms}. On the other hand, according to Eq.8, 3.4×10^{-13} m_{rms} was obtained for it. They agree very well.

The natural sideband of the displacement signal caused by the artificial mirror angle variations at 250Hz (Fig.3) has the identical spectrum shape to the vertical motion of the transmitted light just behind the mirror which can be interpreted as the beam spot motion on the mirror (Fig.4).

4. SIDEBAND EFFECT II

(1) Theory

More generally, when

$$\theta_1(t) = \int_{-\infty}^{\infty} \Theta_1(f)\, e^{2\pi i f t} df$$

$$\theta_2(t) = \int_{-\infty}^{\infty} \Theta_2(f)\, e^{2\pi i f t} df \quad \cdots (10)$$

The Fourier transformation of the cavity length L(f) is, from Eq.3

$$L(f)_{f\neq 0} = \int_{f'<f''} \int D_1(f')\Theta_1(f'')\delta(f'+f''-f)df'df''$$
$$+ \int_{f'<f''} \int D_2(f')\Theta_2(f'')\delta(f'+f''-f)df'df''. \quad \cdots (11)$$

where D_1 and D_2 are the Fourier transformation of the distance between the beam axis and the center mass M_1 and M_2, respectively, and $\delta(\ )$ is the delta function.

Equation 11 indicates that the cavity length change consists of not only the linear effect but also the sum of the sideband effect. When D(f) or Θ(f) at low frequencies is dominant, it roughly follows from Eq.11 that the ratio between the linear effect and the sideband effect at high frequencies is the ratio between d_{st} and d_{rms}, where d_{st} and d_{rms} represents the static offset and the root-mean-square distance between the beam axis and the center mass. Therefore the sideband effect is negligible as compared with the linear effect when $d_{st} >> d_{rms}$.

(2) Experiment

Monochromatic angle jitter at 250Hz and broadband angle jitter (200–315Hz) were artificially caused separately. Their rms motion at 250 Hz with a bandwidth of 1.87Hz were set the same. The corresponding interferometer outputs with d_{st} of 3.1mm and that of 0.1mm are shown in Fig.5 and 6, respectively.

In Fig.5, the monochromatic signal at 250Hz coincides the broadband signal there, which means that the sideband effect is negligible as compared with the linear effect with d_{st} of 3.1mm, whereas some deviations between them as well as ragged broadband signal in Fig. 6 indicates that the sideband effect cannot be neglected with d_{st} of 0.1mm.

On the other hand, the natural rms motion of the beam spots on the mirror was measured to be 0.3mm. Those results are consistent with the theory.

5. PREDICTED ORIENTATION NOISE

The predicted noise of Huey tilt fluctuations caused by the orientation control system with d_{st} of 1mm is shown in Fig. 7 with the typical strain spectrum.

The prediction for each mass at 300Hz is also shown in Table.2. Some of them are more than the current shot noise of the interferometer (3×10^{-19}m/rHz) and even close to the existing noise (1×10^{-16}m/rHz).

Table 2 Predicted orientation noise for each mass at 300Hz.

Test Mass	Coil Voltage (V/rHz)	Diplacement (m/rHz)
Huey (Tilt)	1×10^{-7}	2×10^{-17}
(Rotation)	2×10^{-6}	5×10^{-17}
Louie (Tilt)	6×10^{-8}	4×10^{-20}
(Rotation)	$< 1\times10^{-6}$	$< 9\times10^{-20}$ *
H-Newey (Tilt)	6×10^{-6}	4×10^{-17}
(Rotation)	8×10^{-7}	8×10^{-19} *
L-Newey (Tilt)	1×10^{-7}	1×10^{-18}
(Rotation)	8×10^{-8}	1×10^{-19} *

* Mechanical coupling between tilt and rotation of 15% (measured for Huey) was supposed.

6. CONCLUSION

(1) The model was verified very well.

(2) The orientation control system should be improved.

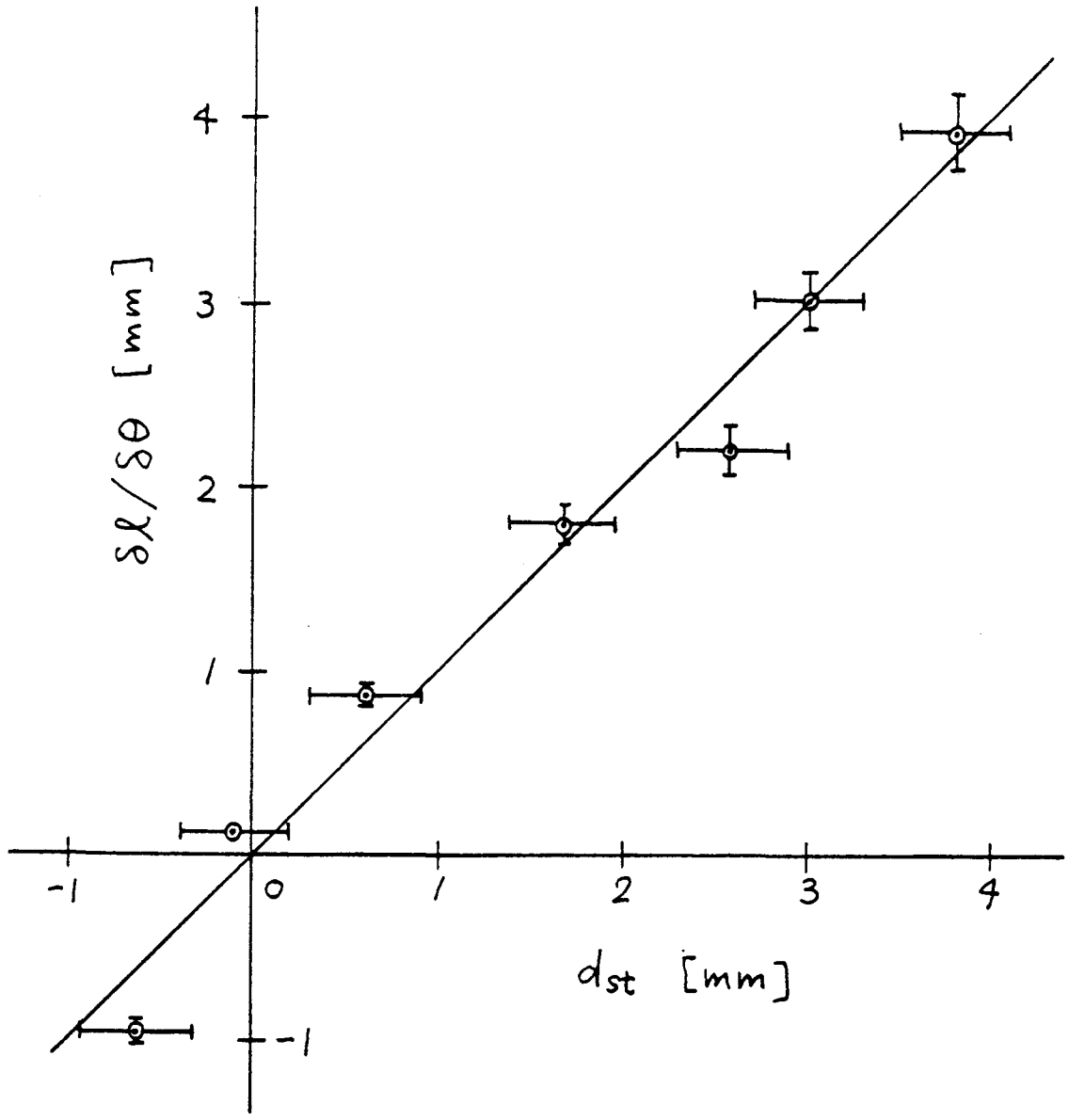

Fig. 2 Linear effect of mirror angle – displacement coupling as a function of static beam spot position. The solid line is $\delta\ell/\delta\theta = d_{st}$

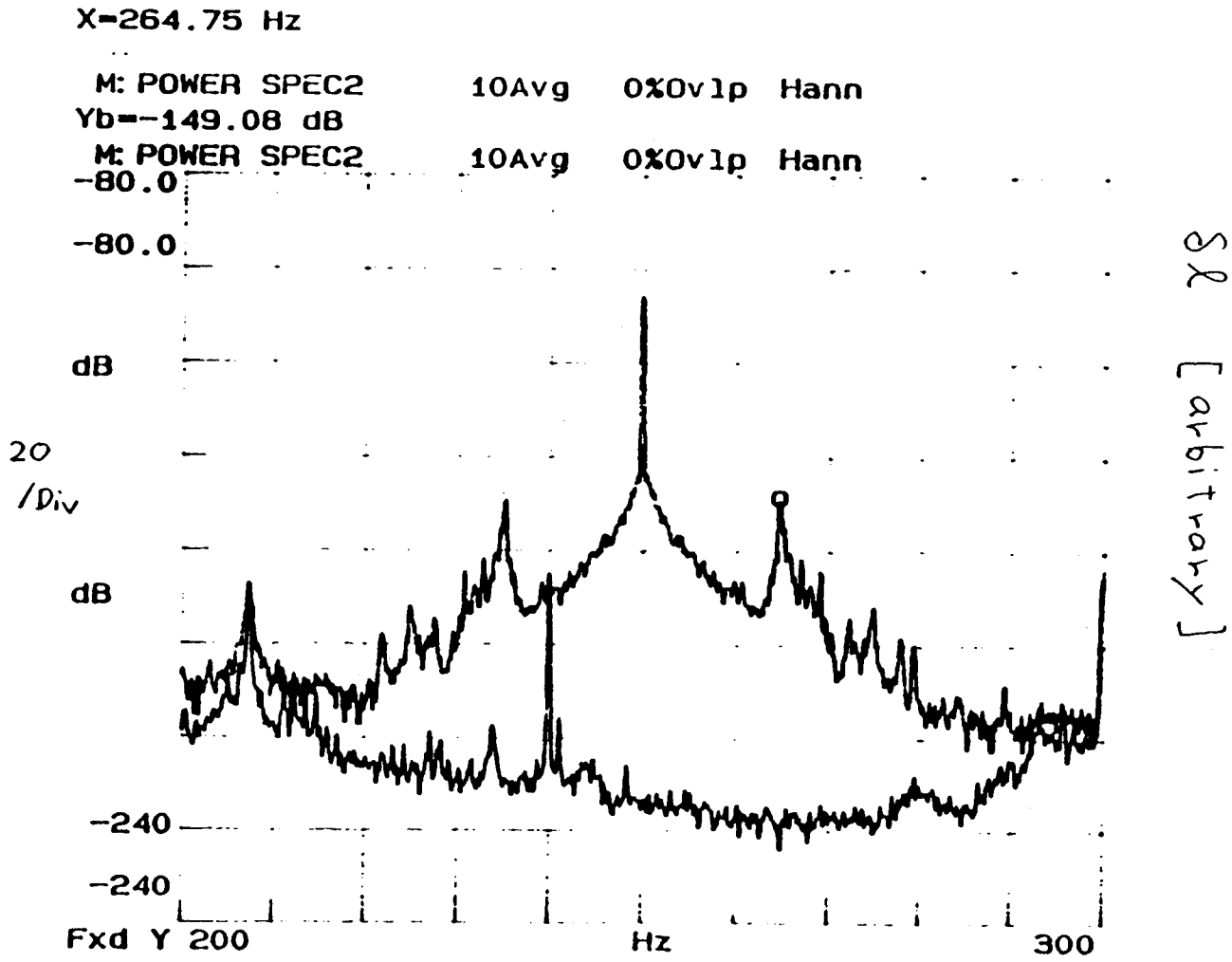

Fig. 3 Displacement spectrum.

Upper : with angle variations at 250 Hz

Lower : natural

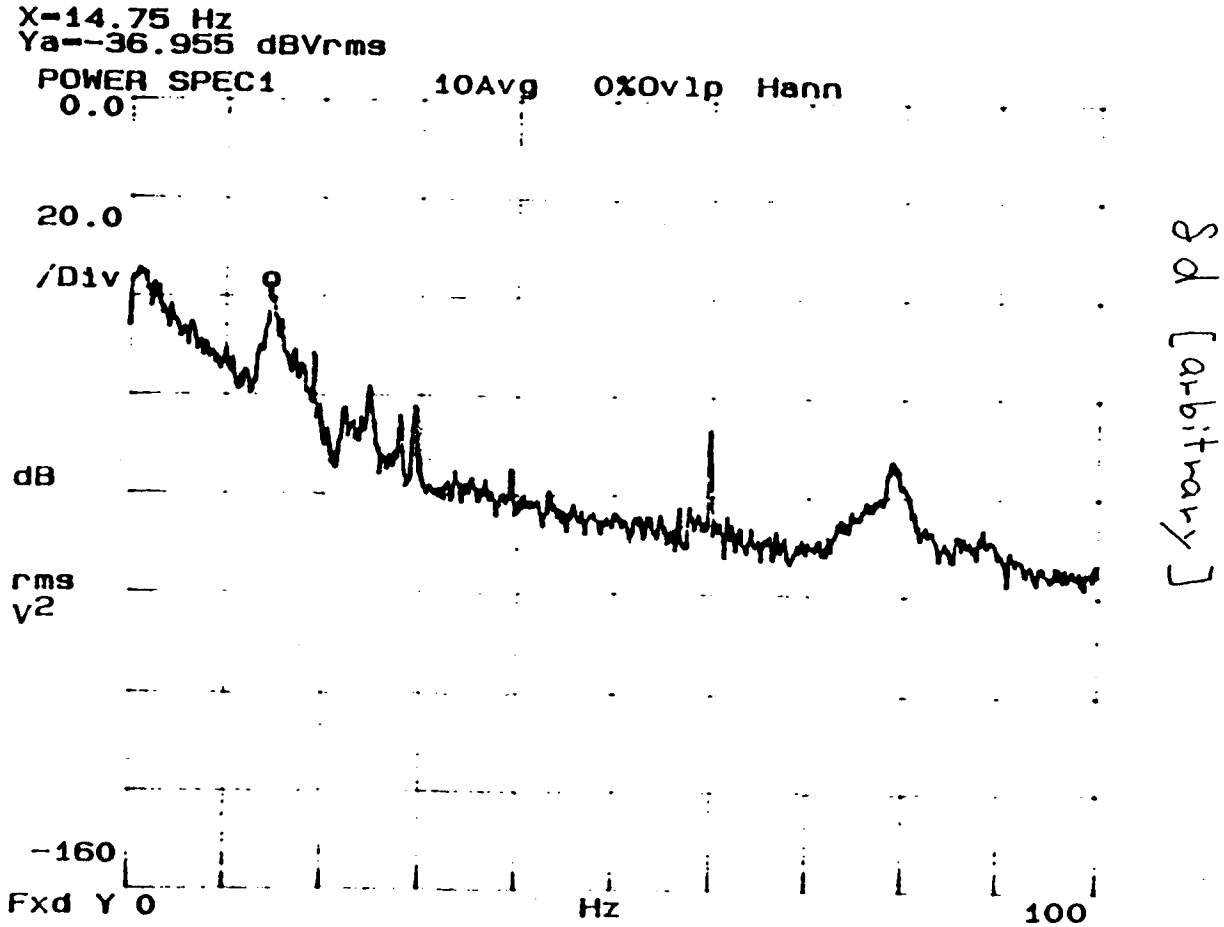

Fig. 4 Beam spot position fluctuation.

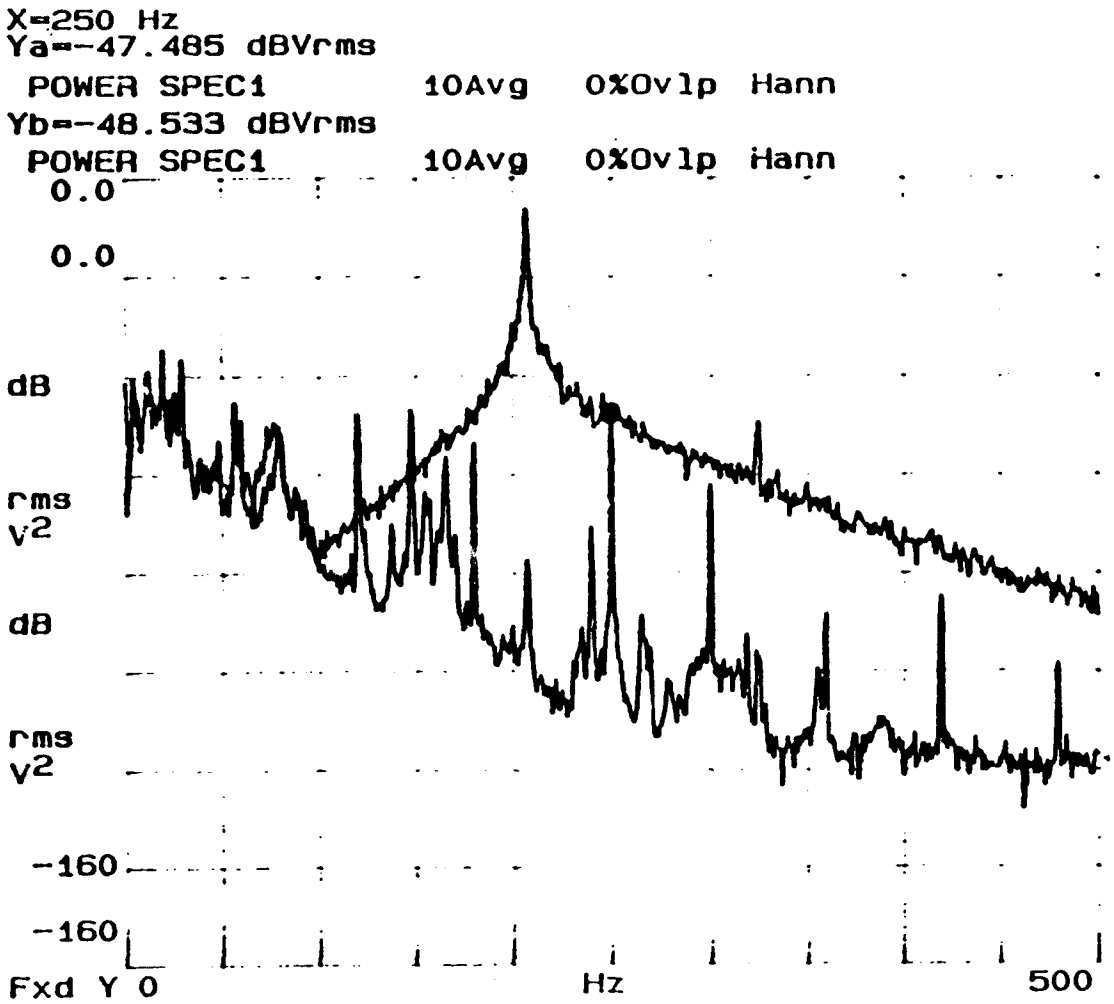

Fig. 5 Uncalibrated displacement spectrum (d_{st} = 3.1 mm)
Upper : with broadband angle variations (200 ~ 315 Hz)
Lower : with monochromatic angle variations (at 250 Hz)

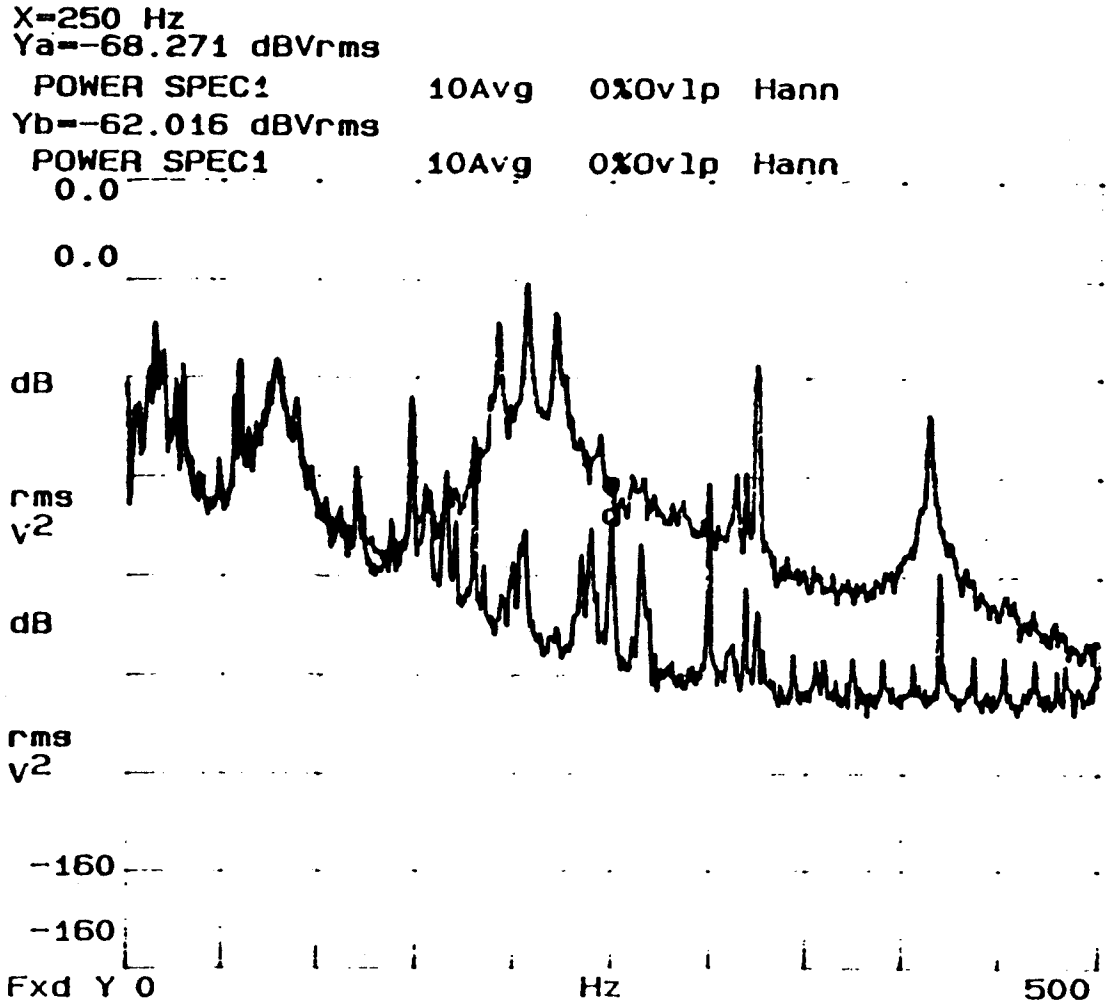

Fig. 6 Uncalibrated displacement spectrum ($d_{s_t} = 0.1\,mm$)
Upper: with broadband angle variations (200 ~ 315 Hz)
Lower: with monochromatic angle variations (at 250Hz)

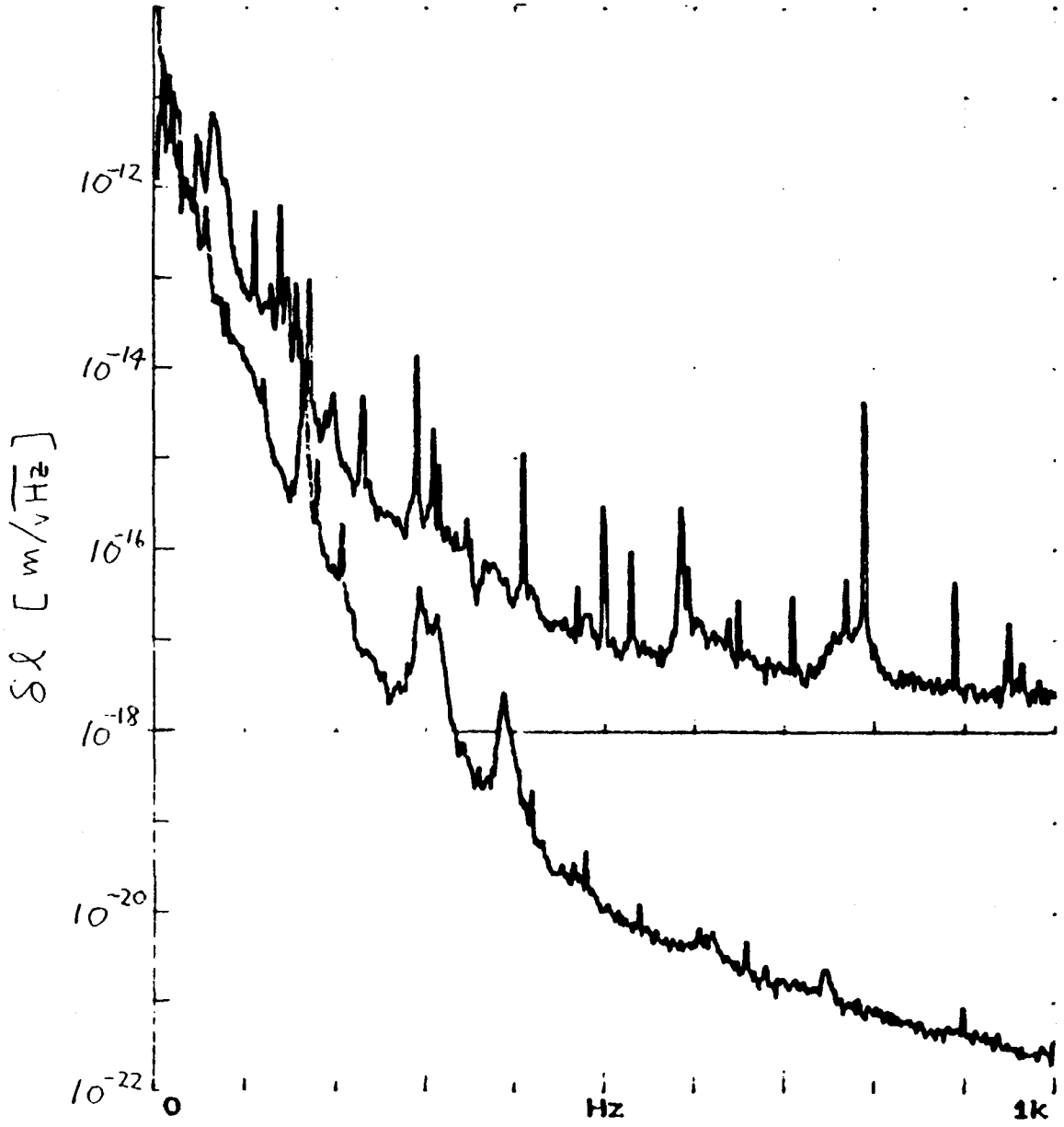

Fig. 7 Predicted orientation noise of Huey tilt (Lower) and typical displacement noise of the 40m prototype (Upper)